Full Title
Oxygen Challenge MR Imaging in Healthy Human Volunteers

Authors
Krishna A. Dani[1], Fiona C. Moreton[1], Celestine Santosh[2], Rosario Lopez[3], David Brennan[3], Christian Schwarzbauer[4], Colin Goutcher[5], Kevin O'Hare[5], I Mhairi Macrae[6], Keith W. Muir[1]

[1]Institute of Neuroscience and Psychology, College of Medical Veterinary and Life Sciences, University of Glasgow, Queen Elizabeth University Hospital Glasgow, 1345 Govan Road, Glasgow G51 4TF
[2]Department of Neuroradiology, Institute of Neurological Sciences, Queen Elizabeth University Hospital Glasgow, Glasgow
[3] Department of Clinical Physics, Institute of Neurological Sciences, Queen Elizabeth University Hospital Glasgow, Glasgow
[4] University of Applied Sciences Munich, School of Applied Sciences & Mechatronics Lothstraße 34 München, DE 80335
[5]Department of Anaesthetics, Institute of Neurological Sciences, Queen Elizabeth University Hospital Glasgow, Glasgow
[6] Institute of Neuroscience and Psychology, College of Medical Veterinary and Life Sciences, Garscube Campus, Glasgow G61 1QH

Correspondence
Professor Keith Muir
SINAPSE Professor of Clinical Imaging & Consultant Neurologist
Institute of Neuroscience & Psychology
University of Glasgow
Queen Elizabeth University Hospital Glasgow, Glasgow G51 4TF
Tel +44 (0)141 201 1100
keith.muir@glasgow.ac.uk

Funding
This project was funded by a project grant award from the Chief Scientists Office Scotland (CSO, ETM/104)

Running Headline
Oxygen Challenge MR Imaging in Volunteers

Word Count
3833 words

Abstract

Oxygen-challenge imaging (OCI) involves transient hyperoxia applied during deoxyhemoglobin sensitive (T2*-weighted) magnetic resonance imaging (MRI), and has the potential to detect changes in brain oxygen extraction. In order to develop optimal practical protocols for OCI, we investigated the influence of oxygen concentration, cerebral blood flow change, pattern of oxygen administration and field strength on T2*-weighted signal. Eight healthy volunteers underwent multi-parametric MRI including OCI and arterial spin labelling (ASL) using two oxygen concentrations (target FiO_2 of 100% and 60%) administered consecutively (two-stage challenge) at both 1.5T and 3T. There was a greater signal increase in grey matter compared to white matter during OC ($p<0.002$ at 3T, $P<0.0001$ at 1.5T) and at FiO_2=100% compared to FiO_2=60% in grey matter at both field strengths ($p<0.02$) and in white matter at 3T only ($p=0.0314$). Differences in the magnitude of signal change between 1.5T and 3T did not reach statistical significance. Reduction of T2*-weighted signal to below baseline, after hyperoxia withdrawal, confounded interpretation of two-stage OCI. Reductions in cerebral blood flow did not obscure the T2*-weighted signal increases. In conclusion, the optimal protocol for further study should utilise target FiO_2=100% during a single oxygen challenge. Imaging at both 1.5T and 3T is clinically feasible.

Key Words

Magnetic Resonance Imaging

Oxygen Challenge Imaging

Hyperoxia

Metabolism

Cerebral Blood Flow

Background

Respiratory challenge using transient inhalation of supplemental gas mixtures during magnetic resonance (MR) imaging may be a useful method to probe the metabolic state of brain tissue. A hyperoxic "challenge" administered whilst scanning with MR sequences sensitive to deoxyhemoglobin (T2*-weighted sequences), precipitates an increase in T2*-weighted signal in healthy tissue, on the basis of a relative decrease in deoxyhemoglobin[1]. Our group has evaluated oxygen challenge imaging (OCI) in rodent models of stroke and in stroke patients[2-8]. In hypometabolic tissue - putative ischaemic core - diminished rises in T2*-weighted signal were observed[4, 8]. In rodent studies the exaggerated rise in T2*-weighted signal intensity in putative ischemic penumbra compared to normal tissue[8] is believed to result from increased deoxyhaemoglobin as a result of increased oxygen extraction fraction (OEF)[9] compared to baseline, and high cerebral blood volume due to compensatory arteriolar vasodilatation.

In this study we sought to;

- Investigate the changes in T2*-weighted signal intensity in response to different inhaled oxygen concentrations
- Compare one-stage oxygen challenge (OCI) to two-stage OCI
- Explore the influence of hyperoxia on cerebral blood flow (CBF), and
- Clarify the feasibility of imaging at different clinically relevant MRI field strengths.

Methods

Simulations

Prior to the human studies, simulations were undertaken to predict T2*-weighted signal change in grey matter in relation to MR field strength, oxygen concentration, and tissue OEF using a previously published method[10]. This is based on a novel biophysical model of blood oxygen level dependant (BOLD) contrast with hyperoxia which accounts for the susceptibility of oxygen dissolved in plasma. This model assumes that the contrast agent does not change the baseline cerebral metabolic rate for oxygen ($CMRO_2$) or OEF of the tissue being investigated.

Subject Recruitment

This study was approved by the West of Scotland Research Ethics Service (REC Reference 12/WS/0200) and written informed consent was attained from all subjects. All experiments were performed in accordance with the Declaration of Helsinki and Good Clinical Practice.

We recruited healthy adult volunteers ≥ 18 years. Exclusion criteria were a. Type II respiratory failure, b. Heart Failure, c. Hemodynamic instability including atrial fibrillation, d. CNS disease likely to affect hemodynamic response to oxygen e.g. previous stroke and e. Contraindications to MR including pregnancy, pacemakers, and ferromagnetic implants.

Study Specific Procedures

Basic demographics and details of medications, vasoactive drug use, and past medical history were recorded. Subjects were scanned using two separate MR scanners (GE Signa) of different field strengths (1.5T and 3T) on two separate days. Prior to scanning, subjects were asked to refrain from ingestion of caffeine or tobacco for 6 hours. Baseline blood pressure, heart rate and nail bed capillary oxygen saturations (SpO_2) were measured using an MR compatible anaesthesia patient monitor (Veris® Vital Signs Monitor, MEDRAD, Indianola, PA).

Gas Administration

Subjects were fitted with an oxygen mask (Intersurgical Ltd, Ref 1141) for the duration of the MR examination. The expiratory ports were closed and used gauze swabs and tape to create a tight seal between the face and the mask. The mask was then connected to a specially designed unidirectional breathing circuit (Ref 2013014, Intersurgical Ltd) via a catheter mount (Intersurgical Ltd, Ref 3514). This prevents rebreathing. The breathing circuit was connected to an anaesthetic machine (Datex Ohmeda Aestiva /5 MRI) via a filter (Clear-Therm 3 HMEF, Luer Lock Port, Intersurgical, Ref 1541). The fraction of inspired oxygen (FiO_2) was varied between 21%, 60%, and 100% in either an ascending or descending sequence during T2*-weighted echoplanar imaging (EPI) and separate arterial spin labelling (ASL) sequences. During the T2*-weighted sequence, medical air was alternated with hyperoxia in the following fashion:

- air (2mins 13s), followed by
- oxygen challenge 1 [OC1] (3mins), followed by
- air (2mins), followed by
- oxygen challenge 2 [OC2] (3mins), followed by
- air (1min).

In half of the subjects (subjects 2,3,6,7) oxygen was given with an FiO_2 = 100% for OC1 and FiO2=60% for OC2 [descending protocol], and the sequence was reversed for the remaining half (subjects 1,5,8,9) [ascending protocol]. Heart rate, respiratory rate and SpO2 were

recorded throughout. Inspired oxygen (FiO_2, %), end tidal carbon dioxide ($ETCO_2$,%) and end tidal oxygen (ETO_2, %) were monitored from a gas sampling line connected to the MedRad monitor.

MRI Protocols

The MR Protocols for the 1.5T and 3T scanners are detailed in Table 1. The protocol for the 3T scanner consisted of a T2*-weighted EPI sequence of 11mins and 12 seconds duration (TR = 2000ms, 332 volumes) as detailed in Table 1. This sequence was acquired with a 30° tilt relative to the AC-PC line in order to reduce artefact from nasal sinuses. The remainder of the 3T examination consisted of 3 pseudocontinuous arterial spin labelling (ASL) sequences acquired with normoxia ($ASL_{21\%}$) and then with the two different levels of hyperoxia in the order given during the EPI sequence ($ASL_{60\%}$ and $ASL_{100\%}$). Parameters for the ASL are also included in Table 1. In addition, for each concentration of oxygen, seven images with fast low shot angle sequences were acquired at different flip angles to allow for correction of the effects of oxygen on T1-weighted signal for the ASL data. A 3D T1-weighted image of the whole brain was also acquired.

Post Processing

Generation of Time Series

A Dell workstation was used for these analyses (Precision T3600, 8GB RAM, Intel Xeon 2.8GHz). The T2*-weighted EPI data acquired at both 3T and 1.5T were realigned to the first image using Statistical Parametric Mapping software (SPM8) which was run using the MATLAB R2013b platform. Next, the 3D T1-weighted imaging (preferably that acquired from the 3T examination) was skull stripped using the FSL Brain Extraction Tool[11]. Maps of grey and white matter were derived using the automated segmentation tool, FAST[12]. Default values were used for this analysis and a binarized map for grey matter and white matter was generated. The skull-stripped original T1-weighted image was transformed and co-registered to the realigned T2*-weighted EPI data using windowed sinc interpolation using Analyze (v8.1, Mayo Clinic, USA). This process required manual manipulation to allow alignment. The transformation matrix was saved and applied to the grey and white matter maps. 'Object maps' delineating grey matter and white matter were overlaid onto the realigned T2*-weighted EPI data in Analyze. The anatomical coverage of the maps was truncated to cover from the level of the basal ganglia to the vertex in order to exclude regions from the posterior fossa. Time series of the raw data were then generated for all volumes of the time series. Wavelet transforms were then applied to smooth the data as

previously described[4], using R software (R Core Team, Vienna 2014; www.R-project.org). The resulting time series data were normalised to the baseline (volumes 0-62) using PRISM software (version 5.04 for Windows, GraphPad Software, San Diego California USA, www.graphpad.com) and area under the curve (AUC) was calculated[4]. The baseline was defined as the mean of volumes 0-62 [0-124s], with AUC for the first oxygen challenge calculated from the data acquired from volumes 73-182 [146-364] (to allow for lag of gas delivery) and the AUC for the second oxygen challenge calculated from the data acquired from volumes 223-332 [446-664s].

Calculation of Change in Cerebral Blood Flow (CBF) and Cerebrovascular Resistance

ASL data were separated into proton density and perfusion images using Image J (Rasband, W.S., ImageJ, U. S. National Institutes of Health, Bethesda, Maryland, USA, http://imagej.nih.gov/ij/, 1997-2014.). The 3D T1-weighted image, $ASL_{FiO2\_21\%}$ and $ASL_{FiO2\_100\%}$ were coregistered to proton density map of $ASL_{FiO2\_21\%}$ with 3D voxel registration using Analyze. The transformed T1-weighted image was skull stripped and segmented using the FSL brain extraction tool and FAST. T1 maps were calculated using MatLab on a pixel-by-pixel basis. The 3D T1-weighted image was segmented into grey matter, white matter and CSF. Binary grey matter masks were generated to extract the T1 values of the grey matter, and an average value for T1 was obtained for each OC for each participant. Quantitative CBF maps were then generated using an in house 'macro' for Image J with correction of T1-weighted signal using the averaged T1 values obtained in the grey matter and with the following equation [operator manual for optima edition 23 based software, GE Healthcare]:

$$CBF = 6000 * \lambda \frac{\left(1-\exp\left(-\frac{ST}{T_{1t}}\right)\right)\exp\left(\frac{PLD}{T_{1b}}\right)}{2T_{1b}\left(1-\exp\left(-\frac{LT}{T_{1b}}\right)\right)\varepsilon * NEX_{PW}}\left(\frac{PW}{SF_{pw}PD}\right)$$

where T1b is T1 of blood and is assumed to be 1.6s at 3T. T1t is the T1 value obtained on grey matter. ST is saturation time and was set to 2s. The partition coefficient λ, is set to the whole brain average, 0.9. The efficiency, ε, is a combination of both inversion efficiency (0.8) and background suppression efficiency (0.75) resulting in an overall efficiency of 0.6. PLD is

the post labelling delay used for the ASL experiment. LT is the labelling duration set to 1.5s. PW is the perfusion weighted or the raw difference image. SFPW is the scaling factor of PW sequence. NEXPW is the number of excitations for PW images. The CBF is reported in units of ml/100g/min.

Binarized grey matter masks were then applied to the $CBF_{21\%}$ map and whole brain grey matter CBF calculated. This was then repeated with the other co-registered ASL scans. To generate measurements of cerebrovascular reactivity the following formula was used in Microsoft Excel: Change in CBF = (Grey matter $CBF_{100\%}$ – Grey matter $CBF_{21\%)}$ / Grey matter $CBF_{21\%}$) * 100. Cerebrovascular reactivity (CVR) was calculated by dividing change in CBF by change in ETO2.

Statistical Analysis

Statistical analyses were performed using StatsDirect software (v2.8.0, Cheshire UK, 2013; www.statsdirect.com). Prior to comparative analyses, normality was assessed using the Shapiro-Wilk test. Paired t-tests or Wilcoxon Signed Ranks Tests were used for normally distributed and non-normally distributed data, respectively. To compare all conditions simultaneously, a two way ANOVA test was employed. To assess the AUC of the T2*-weighted signal change compared to baseline, and the percentage change in CBF compared to baseline, we employed a single sample t-test, using a value of '0' as the baseline comparator. Statistical significance was considered at $p < 0.05$ for two-way tests.

Results

Simulations

Simulations were performed for blood vessels of different sizes at a normal brain oxygen extraction fraction (OEF) of 0.35; data for veins are the most relevant to this study (right hand side of each graph in Figure 1). The predicted T2*-weighted signal change with hyperoxia was modelled for 1.5T and 3T (Figure 1). Simulations for grey matter predicted a greater magnitude of T2*-weighted signal change in response to hyperoxia at 3T compared to 1.5T but a detectable change at 1.5T also. Figure 1 also shows predicted differences in signal response with different concentrations of oxygen, dependent on the underlying tissue OEF. In general, simulations predicted a greater magnitude of T2*-weighted signal change in response to increasing concentrations of oxygen. In penumbral tissue with an OEF of 0.9, higher concentrations of oxygen were predicted to precipitate greater T2*-weighted signal

change, but in hypometabolic tissue (OEF 0.10), a FiO2=100% would precipitate the least T2*-weighted signal intensity owing to the paradoxical effect of paramagnetic oxygen dissolved in plasma.

Subjects

We recruited 9 subjects, one of whom (subject 4) was excluded owing to intolerance of the MR scanner, therefore leaving 8 evaluable subjects. There were five males and three females with median age 35y (range 31-39y). Four subjects were Caucasian, 3 were of South Asian origin, and one of Chinese origin. All subjects were in good health and none was taking vasoactive medications or smoking. Mean blood pressure was 120 (s.d. 11) / 77 (s.d. 11) with oxygen saturations measured by a pulse oximeter of ≥97% in all subjects. The ASL at FiO2=100% was not available for subject 5 since the scan was terminated due to scan intolerance, and ASL could not be analysed for any FiO2 in subject 9 owing to data corruption. We encountered technical problems with the proton density map for subject 8, so we were unable to derive quantitative CBF values for this subject, but we were still able to determine the percentage change in CBF using the CBF maps. Baseline and dynamic data for respiratory parameters and CBF are given in Table 2 and Supplemental Table 1, respectively.

Time Series

Graphs summarising the T2*-weighted signal time series are shown in Figure 2. The T2*-weighted signal increased after oxygen challenge with both FiO_2= 60% and FiO2=100% irrespective of order of administration. Withdrawal of hyperoxia was followed by a decrease in T2*-weighted signal below the original baseline –a post oxygen-challenge (OC) "undershoot" - and remained below the original baseline until the next oxygen challenge or until the sequence finished. Therefore the projected duration of the undershoot beyond 120 seconds after cessation of the OC is unclear.

There was a significant increase in T2*-weighted signal intensity, as measured by AUC, at FiO2=100% in grey matter ($p=0.002$, at 3T; $p<0.0001$, at 1.5T) and white matter ($p=0.007$, at 3T; $p=0.002$ at 1.5T). There was also a significant increase in the AUC of the T2*-weighted signal intensity curve at the lower oxygen concentration of FiO2=60%., both in grey matter

(p=0.001, at 3T; p=0.0003, at 1.5T) and in white matter (p=0.024, at 3T; p=0.02 at 1.5T). There was a highly statistical difference in the AUCs derived under all the different conditions when field strength, tissue type, and oxygen concentration was altered (AUC of T2*-weighted signal intensity curve from grey matter at FiO2=100% at 1.5T, from white matter at FiO2=100% at 1.5T, from grey matter at FiO2=60% at 1.5T, from white matter at FiO2= 60% at 1.5T, from grey matter at FiO2= 100% at 3T, from white matter at FiO2= 100% at 3T, from grey matter at FiO2=60% at 3T, and from white matter at FiO2=60% 3T, p<0.0001, two way ANOVA).

There was a greater T2*-weighted signal change (AUC) precipitated by OC in grey matter compared to white matter (n=8 for all: FiO2=60% at 3T, p=0.0016; FiO2=100% at 3T, p=0.0011; FiO2=60% at 1.5T, p<0.0001; FiO2=100% at 1.5T, p<0.0001). The AUCs during FiO2=100% were greater than those during FiO2=60% in grey matter at both 1.5T and 3T (n=8 for all: p=0.019 at 3T, p=0.0072 at 1.5T) and in white matter at 3T (n=8, p=0.0314) but not at 1.5T (n=8, p=0.177).

There was no statistical difference between the AUCs derived at 1.5T compared to 3T (n=8 for all: for grey matter at FiO2=100%, p=0.72; for grey matter at FiO2=60%, p=0.30; for white matter at FiO2=100%, p=0.77, for white matter at FiO2=60%, p=0.45) in this small sample.

There was no difference between the magnitude of AUCs measured from ascending and descending protocols for FiO2=60% or FiO2=100%.

Cerebral Blood Flow

In grey matter, mean CBF was 51ml/100g/min (s.d 12, n=6, Supplementary Table 1). CBF was lower in all subjects at FiO2=100% (mean CBF =46 ml/100g/min, s.d. 14ml/100g/min; mean reduction = -11%, s.d. 6% [p=0.008, two sided single sample t-test], Figure 3 and Table 2). At FiO2=60%, there was a reduction of CBF in 5 of 7 subjects (mean CBF = 50ml/100g/min , s.d. 14 ml/100g/min; reduction =mean - 3%, s.d. 6%) but this did not reach statistical significance (p=0.23, two sided single sample t-test). The difference in CBF at FiO2=100% compared to FiO2=60% was statistically significant (p=0.005, paired t-test). Neither change in CBF nor change in cerebrovascular resistance significantly correlated with AUC of the T2*-weighted signal at FiO2=100% (CBF, p=0.29; CVR, p=0.07) or at FiO2=60% (CBF, p=0.55; CVR, p=0.85). Figure 3 shows that hyperoxia precipitated a reduction in CBF in subject 1, particularly at FiO_2=100%, and this in turn lead to a reduction in cerebrovascular

resistance (CVR) as shown by the CVR maps. This figure also shows a greater reduction in CBF with 100% O_2 compared to 60% O_2 in subject 1.

Discussion

This study aimed to compare different oxygen delivery protocols for OCI and determine the influence of possible factors confounding T2*-weighted signal change during OCI. The T2*-weighted signal change, as measured by the AUC of the time series of this parameter, was clearly positively influenced by increasing oxygen concentrations, and signal changes were greater in grey matter compared to white matter. This was despite demonstrated reductions in $ETCO_2$, CBF and subsequently CVR which would be expected to attenuate this response. We did not find any evidence of paradoxical decreases in signal intensity, even in white matter. Two-stage OC was confounded by the "undershoot" of T2*-weighted signal after the first oxygen challenge to below baseline. We observed a variable ETO_2 between subjects after delivery of fixed concentration of hyperoxia, despite modifications of the masks to limit gas escape. Finally, OCI is feasible on 1.5T MRI scanners which are more widely available in the clinical setting.

At a FiO_2 of 100% at 3T we observed clearly detectable increases in T2*-weighted signal change in healthy brain tissue. Our finding that OCI induces greater change in T2*-weighted signal in grey matter compared to white matter is expected and reflects greater cerebral metabolic rate for oxygen ($CMRO_2$) and cerebral blood volume in grey matter[13]. Nonetheless, smaller but detectable T2*-weighted signal increases in white matter suggests that OCI may even be able to distinguish normally metabolising from hypometabolic white matter.

Variable inter-subject ETO_2 is expected when a closed gas delivery system (which requires endotracheal intubation or tightly sealed face and nose masks) is impossible within the physical constraints of the head coil combined with subject claustrophobia. In the absence of a specially designed CE marked MRI-compatible mask, we used a standard oxygen mask with additional tape seal, and achieved an ETO_2 of 50-85% at FiO2=100% despite variable subject tolerance, facial geometry and facial hair. Our goal was to evaluate OCI with a clinically compatible system, since this is a key factor in establishing the potential to translate the method to a clinical setting, particularly in acutely unwell patients.

Absolute values for CBF derived from ASL should be interpreted with caution. The measured mean grey matter CBF of 51ml/100g/min is less that one would expect. Global (mean) CBF is accepted to be approximately 50ml/100g/min in young healthy volunteers, as determined

by invasive experimental data[13, 14]. Values for grey matter and white matter cerebral blood flow have been shown to be around 80ml/100g/min and 20ml/100g/min respectively, as determined by intra-arterial Xenon 133 injection techniques[15]. Therefore our technique likely underestimated grey matter CBF. Nonetheless, the observed mean reduction in CBF with hyperoxia of 11%, which was variable among subjects, ranging from 5% to 20% reduction, is consistent with literature reports of a mean reduction of 13-15% in global CBF[13, 14, 16]. Studies using phase contrast MRI have shown slightly greater reductions of up to 27%[17, 18] and one ASL study reported a mean reduction of 32.6%[19]. However, unlike others, our study corrected for the effect of hyperoxia on T1-weighted signal. As in our study, Watson et al showed significant variation of CBF reduction between subjects - 8.99% to 26.7% - using hyperoxia at 15l/min during phase contrast MR[18]. Bulte and colleagues found smaller reductions in CBF using ASL[20] - a mean grey matter CBF reduction of 7% was demonstrated with FiO2=100%, and 4% at FiO2=60%. Our data also reflected this differential effect, with a higher CBF at FiO2=100% compared to FiO2=60%.

The reduction in CBF and CVR due to hyperoxia which was observed in this study, and others, is a potential confounder for our technique. Reductions in CBF are anticipated to reduce T2*-weighted signal intensity, and therefore attenuate rather than exaggerate the T2*-weighted signal intensity increase seen with OCI. We cannot assume similar changes in CBF in those with disease states such as stroke, since autoregulation may be lost, and there may be variability between metabolic tissue compartments within the same subject. Since the CBF changes due to hyperoxia are likely to be due to secondary hypocapnia, a potential solution is to use controlled isocapnic hyperoxia for OCI[21]. Whilst this is feasible for healthy volunteers, it is less practical for patient studies, especially those which study acutely unwell subjects, since sequential gas delivery systems are required. Therefore, if OCI is to become feasible for subjects who are unwell, further study of the magnitude and direction of change in CBF with standard OCI in patients with disordered brain metabolism is desirable, in order to determine potential confounds in such patients.

Since high FiO2 was associated with larger T2* signal changes in healthy brain tissue, this approach is likely to be optimal for future OCI studies. Nonetheless, our current findings relate only to healthy subjects and adaptation of protocols might be appropriate in different disease states. Although under physiological conditions a target FiO2=100% yielded the largest T2*-weighted signal increases, simulations predict different effects of higher oxygen concentration on T2* signal at different OEFs. For example, it was predicted that in tissue with a reduced OEF (0.15), such as might be encountered in infarcted tissue after stroke, the highest oxygen concentration would give rise to the smallest increase in T2*-weighted signal. In practice, this might be due to reduced production of deoxyhaemoglobin secondary to oxidative metabolism, and increased predilection for paramagnetic oxygen to dissolve in plasma which would in turn precipitate a decrease in T2*-weighted signal intensity. This is

consistent with animal experimental stroke data which showed negative changes in T2*-weighted signal within the infarct [22]. It is possible therefore, that the use of more than one oxygen concentration may tease out differences in tissue of varying states of hypometabolic activity. For example, one might hypothesise that the tissue with an increase in T2*-weighted signal intensity during FiO2=60%, but a decrease in signal at FiO2=100% shows more metabolic activity than tissue with negative changes at both oxygen concentrations, and less metabolic activity than tissue with increases at both oxygen concentrations. However, despite the potential attraction of further investigating this hypothesis with the two-stage OC, we noted a post-OC "undershoot". The reduced T2* signal baseline post-oxygen challenge has been observed in rodent studies, both in healthy tissue and to a greater extent in penumbra[2]. Whether this relates to vasomotor or metabolic changes, or a combination, is unclear, but persistent signal change for at least 1600s in rodents, if replicated in humans, makes dual OC impractical in most clinical settings. Potential explanations include rebound increases in CBV or transient increases in OEF as hyperoxia is withdrawn. Regardless of the cause, this change in baseline means that interpretation of the second OCI in our study needs to be cautious.

Finally, we addressed the feasibility of OCI at 1.5T since this field strength is in widest clinical use. The small but non-statistically significant difference in T2*-weighted signal change due to hyperoxia between 1.5T and 3T is consistent with our simulations that predicted lower response at 1.5T compared to 3T. It is also compatible with previously observed lower signal-to-noise ratios at 1.5T compared to 3T and 7T in calibrated Blood Oxygen Level Dependant MRI experiments measuring the cerebral metabolic rate for oxygen[23]. It is possible that a larger number of subjects in our study would have yielded a difference which was statistically significant. Nonetheless, as a result of these data we conclude that although higher field strengths are preferable, OCI is feasible on 1.5T MR scanners, and therefore has the potential to be applied on most clinical MR scanners.

The strengths of this study include the collection of a large number of real time respiratory and MR parameters from the subjects to allow a systematic evaluation of the influences on the OCI signal. In addition, we corrected for the effects of oxygen on T1-weighted signal to reduce confounding of the ASL-derived CBF data. Limitations of this study include the lack of measurement of baseline cerebral blood volume (CBV) or in change in CBV during respiratory challenge. Given that venous CBV is a major influence on T2*-weighted signal, such information would allow a greater understanding of the contributors to the signal attained during OC MRI. Although we did measure the change in CBF and $ETCO_2$, both of which were small, venous CBV measurements during OC MR should be considered in the future, after accurate MR measures of venous CBV have been validated. Next, we made the theoretical assumption that the hyperoxic contrast does not change the baseline metabolic

activity of the tissue. However, this may not actually be the case, and hyperoxia has been shown to reduce peri-infarct depolarisations in experimental models of stroke[24], and lactate production has been shown to be reduced during hyperoxia in human stroke[25]. Therefore, a hyperoxic contrast agent to measure metabolic activity may change the very parameter it is trying to measure, and this represents a potential confound in interpretation of results. Limitations of the application of the oxygen challenge technique included the use of a non-closed system, which gave rise to variable ETO_2 owing to vary degrees of mask fit. In addition, the potentially claustrophobic protocol meant that not all subjects completed the MR examination. We recognise potential challenges in performing this technique in patients who are acutely unwell and may be poorly tolerant of MR imaging. Finally, we also acknowledge the limited numbers of subjects in this study, which could limit statistical power.

For future studies we will apply a single oxygen challenge. If using non-closed respiratory apparatus, we will aim for a FiO2=100%. Although 3T scanners are preferable, the lack of a 3T scanner should not be a barrier. When feasible, one should continue to collect ETO_2 and $ETCO_2$ data as these parameters both may influence OCI results, but there is little suggestion in the available data that CBF changes influence T2* signal response in healthy brain tissue. Creation of a specially designed CE marked mask may be of value for future studies, in order to increase the seal between mask and the face and reduce claustrophobia. In addition, beard shaving may be required if this technique is used in the clinical setting. Future studies should evaluate the influences of hyperoxia on T2*-weighted signal change in subjects with impaired autoregulation and in disease states such as acute stroke, since the effects of hyperoxia on blood flow changes, and in turn T2*-weighted signal, may be different in these cohorts. Specific analysis of the post-OC undershoot should be performed.

Acknowledgements

The authors are grateful to the invaluable input from the stroke research nurses, and neuroradiographers at the Institute of Neurological Sciences, especially Superintendent Isobel Macdonald. We are thankful to the volunteers who participated in this study.

Author Contribution Statement

KD designed the study, contributed to scanning, analysed the data, and wrote the first draft of the manuscript, and modified all subsequent drafts. FM performed much of the scanning, analysed the data, and contributed to all drafts of the manuscript. CS, RL and DB contributed to the design of the study, planned imaging protocols, contributed to

interpretation of the data, and contributed to all drafts of the manuscript. CG and KH contributed to the design of the respiratory aspects of the studies, and reviewed all drafts of the manuscripts. IMM reviewed all drafts of the manuscript. KWM was the senior author and PI of the study, designed the study, and made substantial modifications to all drafts of the manuscript.

Disclosures

None

Supplementary Information

"Supplementary information is available at the Journal of Cerebral Blood Flow & Metabolism website – www.nature.com/jcbfm"

References

1. Ogawa S, Lee TM, Nayak AS, Glynn P. Oxygenation-sensitive contrast in magnetic resonance image of rodent brain at high magnetic fields. *Magn.Reson.Med.* 1990; 14(1)**:** 68.

2. Baskerville TA, Deuchar GA, McCabe C, Robertson CA, Holmes WM, Santosh C *et al.* Influence of 100% and 40% oxygen on penumbral blood flow, oxygen level, and T(2)(star)-weighted MRI in a rat stroke model. *Journal of Cerebral Blood Flow and Metabolism*; 31(8)**:** 1799-1806.

3. Dani KA, Santosh C, Brennan D, Hadley DM, Muir KW. Crossed cerebellar diaschisis: insights into oxygen challenge MRI. *Journal of cerebral blood flow and metabolism : official journal of the International Society of Cerebral Blood Flow and Metabolism* 2012; 32(12)**:** 2114-7.

4. Dani KA, Santosh C, Brennan D, McCabe C, Holmes WM, Condon B *et al.* T2*-weighted magnetic resonance imaging with hyperoxia in acute ischemic stroke. *Ann Neurol* 2010; 68(1)**:** 37-47.

5. Robertson CA, McCabe C, Gallagher L, Lopez-Gonzalez MdR, Holmes WM, Condon B *et al.* Stroke penumbra defined by an MRI-based oxygen challenge technique: 1. Validation using [(14)C]2-deoxyglucose autoradiography. *Journal of Cerebral Blood Flow and Metabolism* 2011; 31(8)**:** 1778-1787.

6. Robertson CA, McCabe C, Gallagher L, Lopez-Gonzalez MdR, Holmes WM, Condon B *et al.* Stroke penumbra defined by an MRI-based oxygen challenge technique: 2. Validation based on the consequences of reperfusion. *Journal of Cerebral Blood Flow and Metabolism* 2011; 31(8)**:** 1788-1798.

7. Robertson CA, McCabe C, Lopez-Gonzalez MR, Deuchar GA, Dani K, Holmes WM *et al.* Detection of ischemic penumbra using combined perfusion and T2* oxygen challenge imaging. *International journal of stroke : official journal of the International Stroke Society* 2015; 10(1)**:** 42-50.

8. Santosh C, Brennan D, McCabe C, Macrae IM, Holmes WM, Graham DI *et al.* Potential use of oxygen as a metabolic biosensor in combination with T2*-weighted MRI to define the ischemic penumbra. *Journal of Cerebral Blood Flow & Metabolism* 2008; 28(10)**:** 1742-53.

9. Baron JC, Bousser MG, Rey A, Guillard A, Comar D, Castaigne P. Reversal of focal "misery-perfusion syndrome" by extra-intracranial arterial bypass in hemodynamic cerebral ischemia. A case study with 15O positron emission tomography. *Stroke* 1981; 12(4)**:** 454-9.

10. Schwarzbauer C, Deichmann R. Vascular component analysis of hyperoxic and hypercapnic BOLD contrast. *Neuroimage* 2012; 59(3)**:** 2401-2412.

11. Smith SM. Fast robust automated brain extraction. *Human Brain Mapping* 2002; 17(3)**:** 143-155.

12. Zhang Y, Brady M, Smith S. Segmentation of brain MR images through a hidden Markov random field model and the expectation-maximization algorithm. *IEEE transactions on medical imaging* 2001; 20(1)**:** 45-57.

13. Kety SS, Schmidt CF. The Effects of Altered Arterial Tensions of Carbon Dioxide and Oxygen on Cerebral Blood Flow and Cerebral Oxygen Consumption of Normal Young Men. *J.Clin.Invest.* 1948; 27(4)**:** 484.

14. Lambertsen CJ, Dough RH, Cooper DY, Emmel GL, Loeschcke HH, Schmidt CF. Oxygen toxicity; effects in man of oxygen inhalation at 1 and 3.5 atmospheres upon blood gas transport, cerebral circulation and cerebral metabolism. *Journal of applied physiology* 1953; 5(9)**:** 471.

15. Ingvar DH, Cronqvist S, Ekberg R, Risberg J, Hoedt-Rasmussen K. Normal values of regional cerebral blood flow in man, including flow and weight estimates of gray and white matter. A preliminary summary. *Acta neurologica Scandinavica. Supplementum* 1965; 14**:** 72-8.

16. Ellingsen I, Hauge A, Nicolaysen G, Thoresen M, Walloe L. Changes in human cerebral blood flow due to step changes in PAO2 and PACO2. *Acta Physiol.Scand.* 1987; 129(2)**:** 157.

17. Rostrup E, Larsson HB, Toft PB, Garde K, Henriksen O. Signal changes in gradient echo images of human brain induced by hypo- and hyperoxia. *NMR in Biomedicine* 1995; 8(1)**:** 41-7.

18. Watson NA, Beards SC, Altaf N, Kassner A, Jackson A. The effect of hyperoxia on cerebral blood flow: a study in healthy volunteers using magnetic resonance phase-contrast angiography. *Eur.J.Anaesthesiol.* 2000; 17(3)**:** 152.

19. Floyd TF, Clark JM, Gelfand R, Detre JA, Ratcliffe S, Guvakov D *et al.* Independent cerebral vasoconstrictive effects of hyperoxia and accompanying arterial hypocapnia at 1 ATA. *J.Appl.Physiol.* 2003; 95(6)**:** 2453.

20. Bulte DP, Chiarelli PA, Wise RG, Jezzard P, Bulte DP, Chiarelli PA *et al.* Cerebral perfusion response to hyperoxia. *Journal of Cerebral Blood Flow & Metabolism* 2007; 27(1)**:** 69-75.

21. Croal PL, Hall EL, Driver ID, Brookes MJ, Gowland PA, Francis ST. The effect of isocapnic hyperoxia on neurophysiology as measured with MRI and MEG. *Neuroimage* 2015; 105**:** 323-31.

22. Shen Q, Huang S, Du F, Duong TQ. Probing ischemic tissue fate with BOLD fMRI of brief oxygen challenge. *Brain research* 2011; 1425**:** 132-41.

23. Hare HV, Blockley NP, Gardener AG, Clare S, Bulte DP. Investigating the field-dependence of the Davis model: Calibrated fMRI at 1.5, 3 and 7T. *Neuroimage* 2015; 112**:** 189-96.

24. Shin HK, Dunn AK, Jones PB, Boas DA, Lo EH, Moskowitz MA *et al.* Normobaric hyperoxia improves cerebral blood flow and oxygenation, and inhibits peri-infarct depolarizations in experimental focal ischaemia. *Brain : a journal of neurology* 2007; 130(Pt 6)**:** 1631.

25. Singhal AB, Ratai E, Benner T, Vangel M, Lee V, Koroshetz WJ *et al.* Magnetic resonance spectroscopy study of oxygen therapy in ischemic stroke. *Stroke* 2007; 38(10)**:** 2851.

1.5T	Duration	TR (ms)	TE (ms)	TI (ms)	SG(ms)	ST (ms)	FA (ms)
3D T1-weighted image - IR-FSPGR	1m43s	2162.3	21.056	750	1.4	1.4	10
T2*-weighted sequence	11m13s	2000	22.4	*	3.5	3.5	80
3.0T							
3D T1-weighted image - BRAVO	4m2s	8.992	3.604	450	1.2	1.2	12
T2-weighted FLAIR	3m20s	10000	144.072	2250	6.5	5	90
T2*-weighted sequence	11m12s	2000	18.9	*	3.5	3.5	80
ASL during normoxia (NEX=3)	4m42s	4864	10.076	2025	3.5	3.5	155
T1 Mapping during concentration during normoxia	54s	5	0.8	*	2	2	-20,2,4,6,8,30
ASL during first oxygen concentration (NEX=3)	4m42s	4864	10.076	2025	3.5	3.5	155
T1 Mapping (SPGR) during first oxygen concentration	54s	5	0.8	*	2	2	-20,2,4,6,8,30
ASL during second oxygen (NEX=3)concentration	4m42s	4864	10.076	2025	3.5	3.5	155
T1 Mapping during second oxygen concentration	54s	5	0.8	*	2	2	-20,2,4,6,8,30

Table 1. Details of MR Protocols at 1.5T and 3T

ms= milliseconds, m=minutes, s=seconds, 3D = three dimensional, IR-FSPGR = fast Spoiled Grass Sequence with inversion recovery preparation, BRAVO = brain volume imaging, FLAIR = fluid-attenuated inversion recovery, ASL = arterial spin labelling, NEX = number of excitations, SPGR = spoiled gradient echo.

	FiO_2	ETO_2 (%)	Change in ETO_2 (%)	$ETCO_2$ (%)	Change in ETCO2 (%)	CVR	Change in CBF (%)	AUC
	Target FiO_2=100%							
Subject 1(a)	99	75	57	4.7	-0.4	-0.35	-20	114
Subject 2(d)	100	60	43	4	-0.6	-0.38	-16	52
Subject 3(d)	95	55	38	5.2	-0.2	-0.15	-6	86
Subject 5 (a)	95	64	47	4.3	-0.4	*	*	115
Subject 6(d)	100	85	68	5	-0.2	-0.07	-5	203
Subject 7(d)	100	83	65	4.7	-0.2	-0.09	-6	145
Subject 8(a)	96	56	40	4.5	-0.1	-0.33	-13	40
Subject 9(a)	95	50	34	5.3	-0.3	*	*	31
Mean (s.d.)	98 (3)	66 (13.4)	49 (13)*	4.7 (0.45)	-0.3 (0.16)**	-0.23 (0.14)**	-11 (6)**	98 (58)*
	Target FiO_2= 60%							
Subject 1(a)	61	47	29.3	4.8	-0.3	-0.31	-9	64
Subject 2(d)	61	34	17	4.6	0	-0.47	-8	49
Subject 3(d)	60	36	19	5.2	-0.2	-0.21	-4	29
Subject 5(a)	64	46	29	4.4	-0.3	-0.20	-6	84
Subject 6(d)	58	44	27.1	5	-0.2	0.07	2	56
Subject 7(d)	60	50	32.6	4.8	-0.1	0.25	8	40
Subject 8(a)	59	34	17.6	4.6	0	-0.28	-5	31
Subject 9(a)	61	33	17	5.5	-0.1	*	*	6
Mean (s.d.)	61 (2)	41 (7)	24 (6.5)*	4.9 (0.36)	-0.15 (0.12)**	-0.17 (0.24) ł	-3 (6)ł	45 (23*)

Table 2. Summary of results for all subjects.

Data acquired at a target FiO_2=100% is given in the top section, and data acquired at a target of FiO_2= 60% is given in the lower section. CVR = cerebrovascular resistance measured in units of (% ΔCBF / % ΔEtO_2) where Δ = change. s.d. = standard deviation. FiO_2 = fractional inspired oxygen, CBF = cerebral blood flow, $ETCO_2$ = end tidal carbon dioxide, ETO_2 = end tidal oxygen, AUC = area under the curve of the T2*-weighted signal intensity curve at 3T. (a) indicates ascending protocol, and (d) indicates descending protocol. * indicates a statistically significant increase compared to baseline conditions, ** indicates a statistically significant decrease compared to baseline conditions, and ł indicates where there was no statistically significant change compared to baseline conditions

	CBF (ml/100g/min)	ETO_2 (%)	$ETCO_2$ (%)
		Baseline	
Subject 1	37	18	5.1
Subject 2	50	17	4.6
Subject 3	40	17	5.4
Subject 5	53	17	4.7
Subject 6	71	17	5.2
Subject 7	55	17	4.9
Subject 8	*	16	4.6
Subject 9	*	16	5.6
Mean (s.d.)	51 (12)	17 (0.6)	5 (0.4)

Supplemental Table 1. Baseline measurements from all subjects breathing air.

Note that subject 4 did not tolerate any imaging and was therefore not included. Baseline CBF data were not available for subject 8 owing to technical issues with the proton density map, and CBF data were not available for subject 9. CBF = cerebral blood flow. ETO_2 = end tidal oxygen, $ETCO_2$ = end tidal carbon dioxide

Titles and legends to figures

Figure 1. Dependence of T2*-weighted signal change on field strength, gas type and Oxygen Extraction Fraction (OEF).

The figure shows simulations for the dependence of brain T2*-weighted signal change (% change relative to air) (y-axis) as a function of vessel diameter, vessel type, OEF and field strength. Data to the left of the first broken vertical line correspond to arteries, data between the vertical broken lines correspond to capillaries, and data to the right of the second vertical line correspond to veins. The diameter of vessels increases along the x-axis from the middle section (which represents the smallest vessels [capillaries]) in a leftward and rightward direction. Data from different gas types are colour coded according to the figure key. The top panel shows simulations which assume a normal OEF (0.35) at 1.5T, and the effect of field strength can be seen when comparing to the simulations for the same OEF at 3.0T, in the graph directly below it. The bottom panel shows the effect of changing OEF on T2*-weighted signal at 3.0T, with OEF increasing from left to right. The graph on the left shows data from a low OEF (0.10) as might be seen in infarct core, the middle graph shows a normal OEF and the graph on the right shows data from 'penumbral' OEF (0.9).

Figure 2. T2*-weighted signal intensity curves.

Data from both 3T (top) and 1.5T (bottom) in both grey matter (left column) and white matter (right column) are shown, with data from ascending and descending protocols shown separately. In four subjects the oxygen was given with a FiO_2 =100% for OC1 and

FiO_2=60% for OC2 [descending protocol], and the sequence was reversed for a second cohort of 4 subjects [ascending protocol]. The solid line data points show the mean data from 4 subjects and the grey lines show standard deviations. Broken vertical lines show the onset and offset of the first oxygen challenge, and the solid vertical lines show the same for the second oxygen challenge.

Figure 3. Blood Flow and Cerebrovascular Resistance Maps

Top panel show maps of cerebral blood flow (CBF) at FiO_2 of 21%, 60%, and 100% from subject 1, running from left to right. The color scale indicates cerebral blood flow (ml/100g/min). The bottom panel shows cerebrovascular reactivity (CVR) maps from subject 1 when alternating between FiO2 of 21% and 60% (bottom left) and between FiO2 21% and 100% (bottom right). The color scale indicates percentage change in cerebral blood flow (the '-' sign indicates a reduction in cerebral blood flow) The maps show a reduction in cerebral blood flow with hyperoxia, which is more pronounced at FiO2 100% compared to FiO2 60%. The colour scale shows CVR (%).

Figure 1

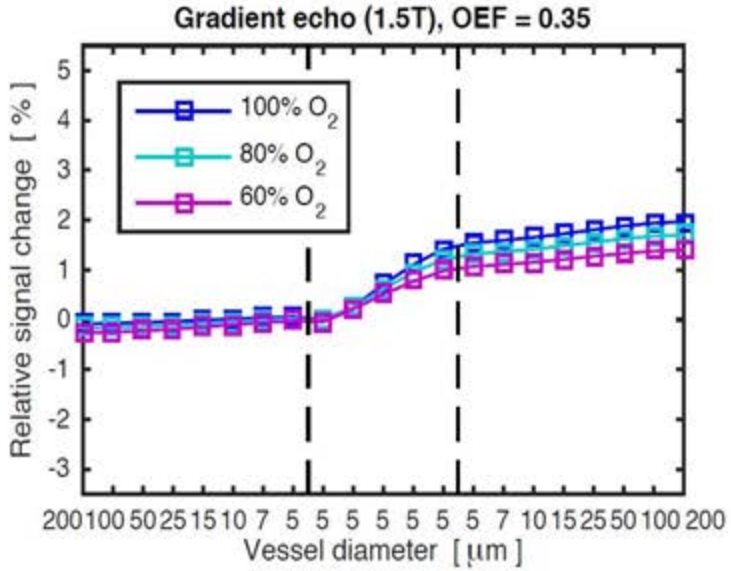
Gradient echo (1.5T), OEF = 0.35
Relative signal change [%]
100% O2
80% O2
60% O2
Vessel diameter [µm]

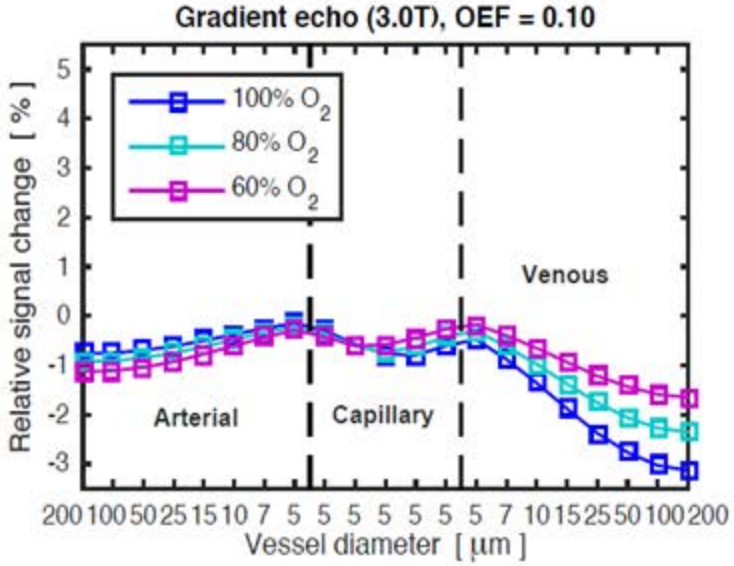
Gradient echo (3.0T), OEF = 0.10
Relative signal change [%]
100% O2
80% O2
60% O2
Arterial
Capillary
Venous
Vessel diameter [µm]

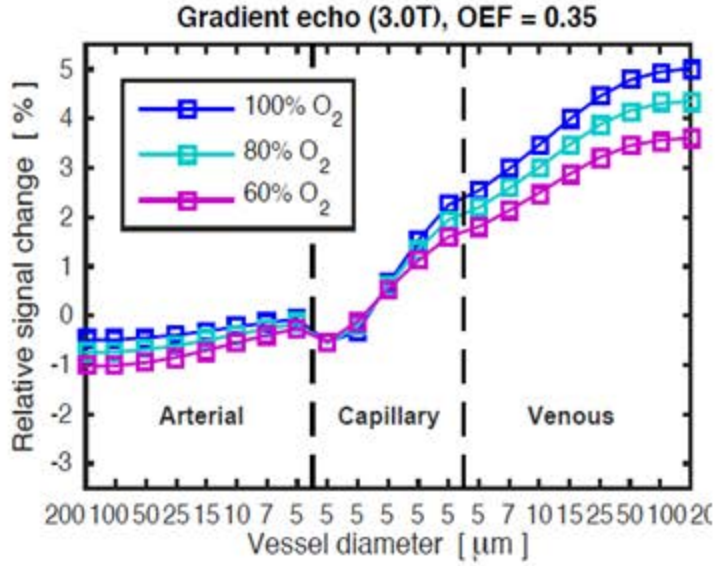
Gradient echo (3.0T), OEF = 0.35
Relative signal change [%]
100% O2
80% O2
60% O2
Arterial
Capillary
Venous
Vessel diameter [µm]

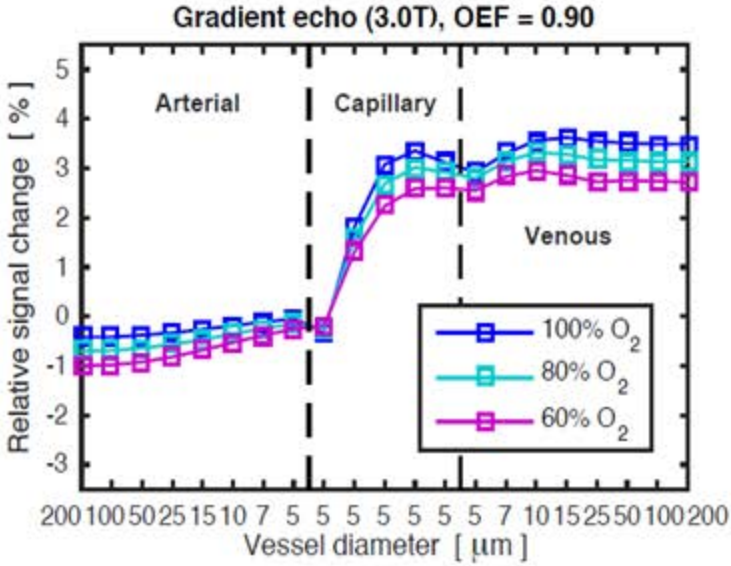
Gradient echo (3.0T), OEF = 0.90
Relative signal change [%]
Arterial
Capillary
Venous
100% O2
80% O2
60% O2
Vessel diameter [µm]

Figure 2

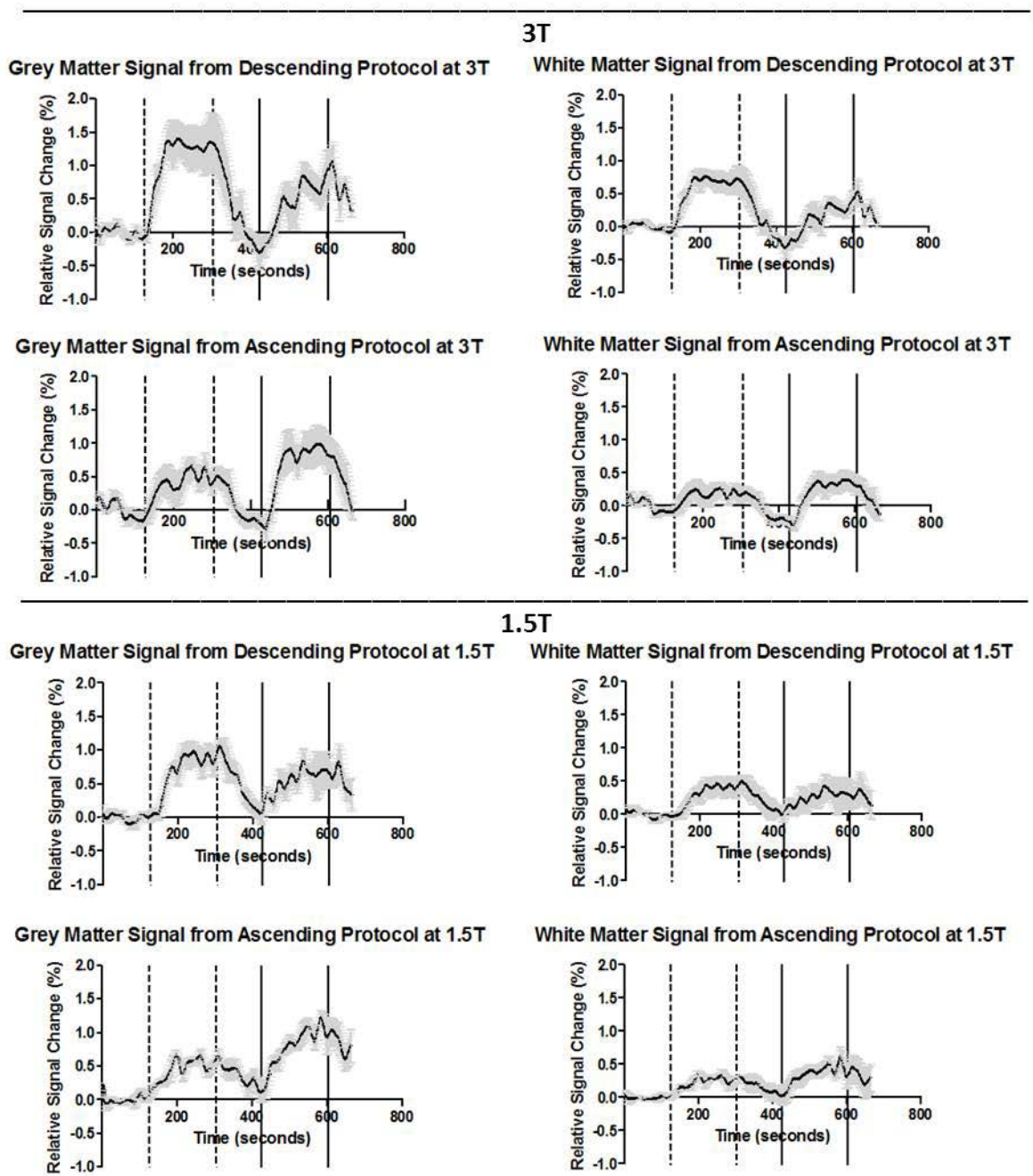
Grey Matter
White Matter
3T
Grey Matter Signal from Descending Protocol at 3T
White Matter Signal from Descending Protocol at 3T
Grey Matter Signal from Ascending Protocol at 3T
White Matter Signal from Ascending Protocol at 3T
1.5T
Grey Matter Signal from Descending Protocol at 1.5T
White Matter Signal from Descending Protocol at 1.5T
Grey Matter Signal from Ascending Protocol at 1.5T
White Matter Signal from Ascending Protocol at 1.5T
Relative Signal Change (%)
Time (seconds)

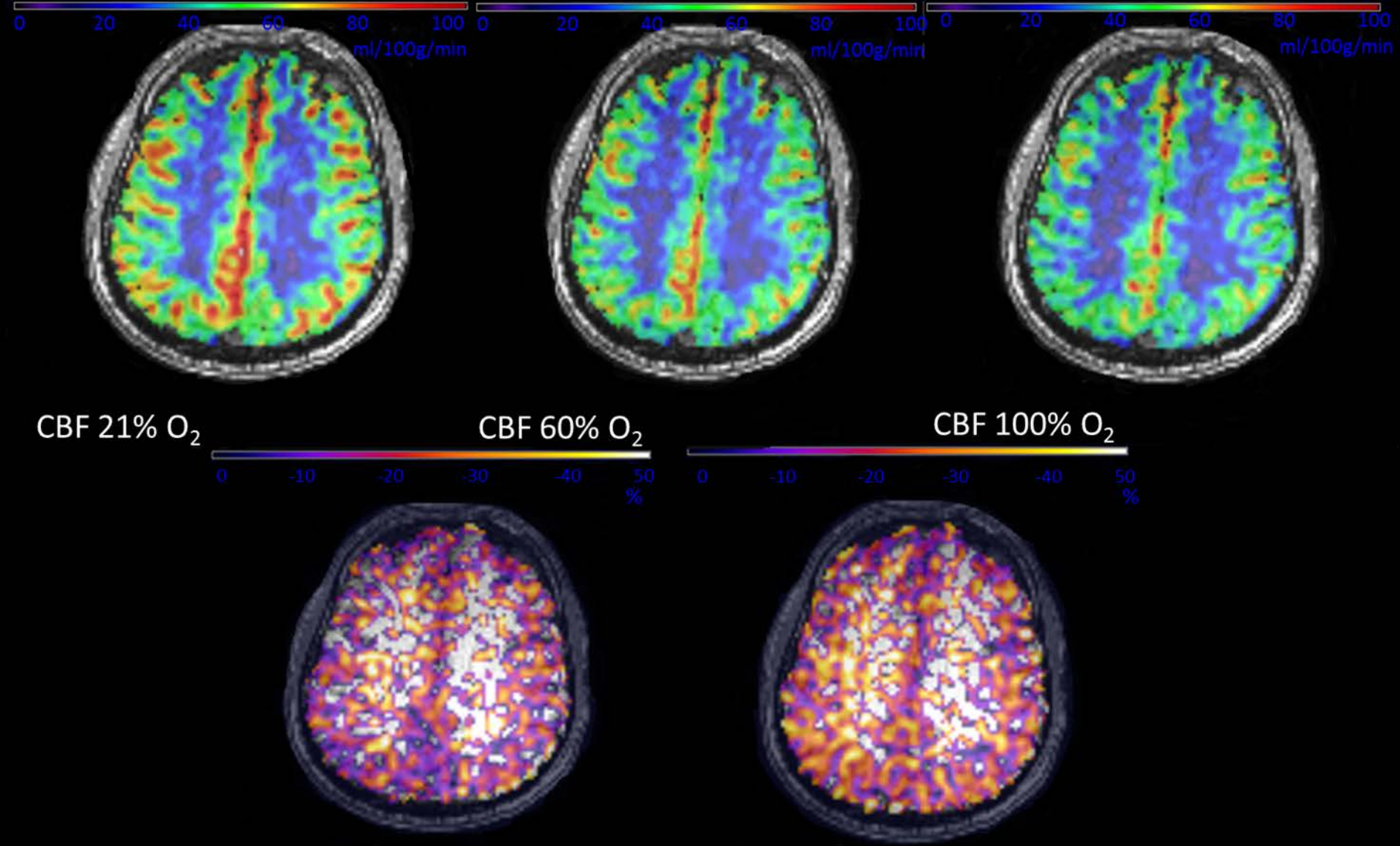
0 20 40 60 80 100
ml/100g/min
0 20 40 60 80 100
ml/100g/min
0 20 40 60 80 100
ml/100g/min
CBF 21% O2
CBF 60% O2
CBF 100% O2
0 -10 -20 -30 -40 50
%
0 -10 -20 -30 -40 50
%
CVR 21% / 60% O2
CVR 21% / 100% O2

Figure 3